



Dielectric properties of oxygen post-annealed $\text{Cu}_{0.5}\text{Tl}_{0.5}\text{Ba}_2\text{Ca}_3(\text{Cu}_{4-y}\text{Cd}_y)\text{O}_{12-\delta}$ bulk superconductor

M. Mumtaz^{a,b,*}, M. Rahim^b, Nawazish A. Khan^b, K. Nadeem^a, Khurram Shehzad^c

^aMaterials Research Laboratory, Department of Physics FBAS, International Islamic University (IIU), Islamabad 44000, Pakistan

^bMaterials Science Laboratory, Department of Physics, Quaid-i-Azam University, Islamabad 45320, Pakistan

^cDepartment of Engineering Mechanics, Center for Nano and Micro Mechanics, Tsinghua University, Beijing 100084, China

Received 25 March 2013; received in revised form 8 May 2013; accepted 8 May 2013

Available online 25 May 2013

Abstract

Oxygen post-annealing experiments are carried out to optimize the oxygen contents in $\text{Cu}_{0.5}\text{Tl}_{0.5}\text{Ba}_2\text{Ca}_3(\text{Cu}_{4-y}\text{Cd}_y)\text{O}_{12-\delta}$ ($y=0, 0.25, 0.5,$ and 0.75) superconductor samples and to investigate its effects on their dielectric properties {i.e. dielectric constants ($\epsilon'_r, \epsilon''_r$), absolute dielectric loss $|\tan \delta|$ and ac-conductivity (σ_{ac})}. The negative capacitance (NC) is observed in all post-annealed $\text{Cu}_{0.5}\text{Tl}_{0.5}\text{Ba}_2\text{Ca}_3(\text{Cu}_{4-y}\text{Cd}_y)\text{O}_{12-\delta}$ samples. Almost all the dielectric properties are suppressed except dielectric loss ($\tan \delta$), which is increased after oxygen post-annealing. The appreciable change in the dielectric properties is the indication of oxygen intake by $\text{Cu}_{0.5}\text{Tl}_{0.5}\text{Ba}_2\text{Ca}_3(\text{Cu}_{4-y}\text{Cd}_y)\text{O}_{12-\delta}$ samples after oxygen post-annealing. The thermal agitation is higher and polarizability is lower at normal state (300 K), resulting in decrease of the dielectric constant and increase in $\tan \delta$ which is vice versa at lower temperatures. The observed variation in the dielectric behavior of $\text{Cu}_{0.5}\text{Tl}_{0.5}\text{Ba}_2\text{Ca}_3(\text{Cu}_{4-y}\text{Cd}_y)\text{O}_{12-\delta}$ samples strongly depends on the working (or operating) temperature and frequency of the external applied ac-field. The dielectric behavior of the material can be regulated by the post-annealing in oxygen as a result of which the variation of oxygen content of the materials structures may take place thus changing the carrier's density. On the other hand, this post-annealing may affect the inter-grain connectivity of the materials that can influence the dielectric properties of the material.

© 2013 Elsevier Ltd and Techna Group S.r.l. All rights reserved.

Keywords: $\text{Cu}_{0.5}\text{Tl}_{0.5}\text{Ba}_2\text{Ca}_3(\text{Cu}_{4-y}\text{Cd}_y)\text{O}_{12-\delta}$ superconductor; Negative capacitance; Dielectric properties; Post-annealing

1. Introduction

The oxygen content in the charge reservoir layers control the carriers density in CuO_2 planes of multilayered cuprates [1,2]. Oxygen post-annealing is the simple and appropriate way to vary the oxygen contents in the cuprates. The change in O_δ oxygen variation in $\text{Cu}_{0.5}\text{Tl}_{0.5}\text{Ba}_2\text{O}_{4-\delta}$ charge reservoir layer controls the flow of carriers toward the conducting CuO_2 planes of $\text{Cu}_{0.5}\text{Tl}_{0.5}\text{Ba}_2\text{Ca}_3(\text{Cu}_{4-y}\text{Cd}_y)\text{O}_{12-\delta}$ samples. The charge carriers are mobile in the conducting CuO_2 planes, while Tl^{3+} , Cu^{2+} and Ba^{2+} ions localize the charge carriers in $\text{Cu}_{0.5}\text{Tl}_{0.5}\text{Ba}_2\text{O}_{4-\delta}$ charge reservoir layer [3]. The dielectric

constant arises from the accumulation of carriers in between CuO_2 planes and $\text{Cu}_{0.5}\text{Tl}_{0.5}\text{Ba}_2\text{O}_{4-\delta}$ charge reservoir layer. It is well known that there are four primary mechanisms of polarization in materials [3–7] namely electronic polarization (α_e), which can be observed at very high frequencies of the order of 10^{15} Hz (i.e. in ultraviolet optical range), atomic and ionic polarization (α_a), which takes place at the frequencies in range of 10^{10} – 10^{13} Hz (i.e. in the infrared optical range), dipolar or oriental polarization (α_o), which occurs in the range of frequencies from 10^3 to 10^6 Hz (i.e. in the sub-infrared optical range), and interfacial polarization (α_i), which is more sensitive in the low frequency range of 10^3 Hz and may extend to few kilohertz range [8]. Each mechanism of polarization involves a short-range motion of charges and contributes to the total polarization of the material.

The dipolar or oriental polarization and interfacial polarization mainly contribute to the dielectric response of

*Corresponding author at: Materials Research Laboratory, Department of Physics FBAS, International Islamic University (IIU), Islamabad 44000, Pakistan. Tel.: +92 51 9019715; fax: +92 51 9210256.

E-mail address: mmumtaz75@yahoo.com (M. Mumtaz).

$\text{Cu}_{0.5}\text{Tl}_{0.5}\text{Ba}_2\text{Ca}_3(\text{Cu}_{4-y}\text{Cd}_y)\text{O}_{12-\delta}$ superconductor samples because the dielectric constant become saturated in the high frequency range at all temperatures from superconducting state to room temperature. The dipolar polarization or the oriental polarization contributes to the dielectric properties in the sub-infrared range of frequency [3]. Mobile carriers are impeded by a physical barrier in the interfacial polarization that inhibits charge migration. The charges pile up at the barrier producing a localized polarization in the materials [8]. Therefore, all the above mentioned mechanisms of polarization are important at low frequencies however, the effects of dipolar polarization are weak and the dielectric constant mainly originates from electric and lattice polarization contribution on account of their short relaxation time. The conduction mechanisms of variety of electronic devices strongly depend upon the temperature, frequency, fabrication conditions and process, surface charges, doping concentration and impurities (interface states or dislocations). The dielectric properties do not reflect the same intrinsic response at all frequencies and temperatures. Therefore, the study of dielectric properties and ac-conductivity over the wide range of frequency and temperature is very important. The determination of dielectric properties and ac-conductivity of the materials at different frequencies and temperatures can provide valuable information about the conduction and polarization mechanisms. The materials with giant dielectric constant are playing an increasingly significant role in the growth of microelectronics because of the desire for smaller and more robust devices such as capacitor and memory devices [9]. However, the main problem for potential applications is the high conductivity in cuprates, which results in high dissipation loss. The large polarizability of Tl^{3+} , Ba^{2+} and Cu^{2+} ions may contribute to the possible high frequency practical applications of $\text{Cu}_{0.5}\text{Tl}_{0.5}\text{Ba}_2\text{Ca}_3(\text{Cu}_{4-y}\text{Cd}_y)\text{O}_{12-\delta}$ compound. Most importantly, the conductivity can be adjusted in $\text{Cu}_{0.5}\text{Tl}_{0.5}\text{Ba}_2\text{Ca}_3(\text{Cu}_{4-y}\text{Cd}_y)\text{O}_{12-\delta}$ compound to relatively low value by changing the oxygen contents because the oxygen contents in the charge reservoir layer determines the valence state of Tl and Cu that control the carriers density in the conducting CuO_2 planes [10–14]. As is known, very low conductivity is absolutely necessary for low dissipation factor.

In this article, we have reported the frequency dependent dielectric measurements of oxygen post-annealed $\text{Cu}_{0.5}\text{Tl}_{0.5}\text{Ba}_2\text{Ca}_3(\text{Cu}_{4-y}\text{Cd}_y)\text{O}_{12-\delta}$ superconductor in comparison with as-prepared samples. The oxygen post-annealing experiments are normally carried out to modify the chemical state of elements in the unit cell by varying the oxygen contents to optimize the carriers concentration, to increase the grains size and to enhance the inter-grain connectivity in bulk materials [10–14]. Therefore our main objective of oxygen post-annealing experiments on $\text{Cu}_{0.5}\text{Tl}_{0.5}\text{Ba}_2\text{Ca}_3(\text{Cu}_{4-y}\text{Cd}_y)\text{O}_{12-\delta}$ superconductor samples was to optimize the carriers concentration and to increase the grains size as well as to enhance the inter-grain connectivity. The effects of all these factors after oxygen post-annealing can be visualized in the form of variation in the dielectric properties deduced from experimental data of capacitance and conductance measurements at different temperatures and frequencies. We have calculated the dielectric

constants (ϵ'_r , ϵ''_r), absolute dielectric loss $|\tan \delta|$ and ac-conductivity (σ_{ac}) by experimentally measuring the capacitance (C) and conductance (G) with the help of Hewlett-Packard 4275 A Multi-Frequency LCR Meter from 10 KHz to 10 MHz at various temperatures from 80–300 K. We have compared the dielectric properties of post-annealed $\text{Cu}_{0.5}\text{Tl}_{0.5}\text{Ba}_2\text{Ca}_3(\text{Cu}_{4-y}\text{Cd}_y)\text{O}_{12-\delta}$ samples with those of un-annealed as-prepared $\text{Cu}_{0.5}\text{Tl}_{0.5}\text{Ba}_2\text{Ca}_3(\text{Cu}_{4-y}\text{Cd}_y)\text{O}_{12-\delta}$ samples [15]. The capacitance, conductance, dielectric constant, dielectric loss and ac-conductivity are the main parameters for the selection of the materials for device applications. The dielectric parameters (ϵ'_r , ϵ''_r , $|\tan \delta|$ and σ_{ac}) can be determined by means of C and G measurements in the test frequency (f) range of 10 KHz to 10 MHz using the following expressions [16].

The real part of dielectric constant (ϵ'_r) can be calculated by the expression

$$\epsilon'_r = \frac{Cd}{A\epsilon_o} \quad (1)$$

where C is capacitance (F), d is the thickness of the dielectric/separation between the plates of the capacitor (m), ϵ_o is the permittivity of free space ($\epsilon_o = 8.85 \times 10^{-12} \text{ F m}^{-1}$) and A is the area of the electrodes (m^2).

The imaginary part of dielectric constant or dielectric loss (ϵ''_r) of the material can be calculated from the conductance (G) by using the following equation

$$\epsilon''_r = \frac{Gd}{A\epsilon_o\omega} \quad (2)$$

where $\omega (=2\pi f)$ is the angular frequency.

The dielectric loss $\tan \delta$ can be calculated from the relation

$$\tan \delta = \frac{\epsilon''_r}{\epsilon'_r} \quad (3)$$

The ac-conductivity (σ_{ac}) can be calculated by using the following relation

$$\sigma_{ac} = 2\pi f \epsilon_o \epsilon'_r \tan \delta \quad (4)$$

where f is the frequency of the external applied ac-field (Hz).

2. Experimental

The polycrystalline bulk $\text{Cu}_{0.5}\text{Tl}_{0.5}\text{Ba}_2\text{Ca}_3(\text{Cu}_{4-y}\text{Cd}_y)\text{O}_{12-\delta}$ ($y=0, 0.25, 0.5, \text{ and } 0.75$) superconductor samples were synthesized by the solid-state reaction method using $\text{Cd}(\text{NO}_3)_2$, $\text{Ba}(\text{NO}_3)_2$, $\text{Ca}(\text{NO}_3)_2$ and $\text{Cu}(\text{CN})$ as starting compounds. These compounds are mixed in appropriate ratios and ground in a quartz mortar pestle for about an hour and then fired at 880°C in a quartz boat for 24 h followed by furnace cooling to room temperature. This material was again ground for about 1 h and heat-treated at the same temperature of 880°C for 24 h. The fired material was then mixed with Tl_2O_3 and ground again for about 1 h. The material mixed with Tl_2O_3 was palletized under 5 t/cm^2 pressure and the pellets were enclosed in gold capsules for heat-treatment at 880°C for 10 min followed by quenching to room temperature. The bar shaped samples of dimensions $2 \text{ mm} \times 2.5 \text{ mm} \times 10 \text{ mm}$ were used for characterizations. The post-annealing experiments on

these samples were carried out in tubular furnace at 500 °C in flowing oxygen for 6 h. The bar shaped samples of dimensions 2 mm × 2.5 mm × 10 mm were used for dc-resistivity ρ (Ω cm) measurements by the four-probe method. The frequency dependent dielectric measurements were carried out with the help of Hewlett-Packard 4275 A Multi-Frequency LCR Meter in the frequency range of 10 KHz to 10 MHz. The calibrations of the LCR meter were performed with the help of standard capacitor in order to elucidate the influence of an external circuit. The parallel mode of LCR meter was used for these measurements. A conventional two-probe technique was used for the capacitance (C) and conductance (G) measurements of $\text{Cu}_{0.5}\text{Tl}_{0.5}\text{Ba}_2\text{Ca}_3(\text{Cu}_{4-y}\text{Cd}_y)\text{O}_{12-\delta}$ superconductor samples. Silver paint was applied on both the surfaces of the sample and copper leads were fixed on the silver electrode surfaces.

3. Results and discussion

The summary of the comparison of superconductivity and dielectric properties of as-prepared [15] and oxygen post-annealed $\text{Cu}_{0.5}\text{Tl}_{0.5}\text{Ba}_2\text{Ca}_3(\text{Cu}_{4-y}\text{Cd}_y)\text{O}_{12-\delta}$ superconductor samples is given in Table 1.

The x-ray diffraction (XRD) scans of as-prepared $\text{Cu}_{0.5}\text{Tl}_{0.5}\text{Ba}_2\text{Ca}_3(\text{Cu}_{4-y}\text{Cd}_y)\text{O}_{12-\delta}$ ($y=0, 0.25, \text{ and } 0.5$) samples have shown tetragonal structure following P4/mmm space group with a-axes lengths 4.146, 4.146, and 4.147 Å and c-axes lengths 17.86, 17.83, and 17.8 Å for $y=0, 0.25, \text{ and } 0.5$, respectively [17]. The lattice parameters of these samples are calculated by using computer software (crystal). The ionic size of Cd^{2+} (1.41 Å) is large as compared to that of Cu^{2+} (1.17 Å) but the decrease in c-axis length gives the clue of reduced Jahn–Teller distortion with Cd-doping. The non-linear molecules having a degenerate electronic state distort to lower the symmetry of the molecule and reduce the degeneracy. This is commonly known as Jahn–Teller effect and this effect can be observed for partially filled energy level [17]. The dc-resistivity ρ (Ω cm) versus temperature T (K) measurements of oxygen post-annealed $\text{Cu}_{0.5}\text{Tl}_{0.5}\text{Ba}_2\text{Ca}_3(\text{Cu}_{4-y}\text{Cd}_y)\text{O}_{12-\delta}$ superconductor samples are shown in Fig. 1. The variation in resistivity for all these samples from room temperature down to onset of superconductivity is metallic with onset temperature (T_c^{onset}) of superconductivity around 131, 124, 120, and 108 K and zero resistivity critical temperature ($T_c(R=0)$) around 120, 114, 115, and 85 K for $y=0, 0.25, 0.5, \text{ and } 0.75$ respectively. Both the T_c^{onset} and $T_c(R=0)$ are shifted to higher temperature values in all the oxygen post-annealed $\text{Cu}_{0.5}\text{Tl}_{0.5}\text{Ba}_2\text{Ca}_3(\text{Cu}_{4-y}\text{Cd}_y)\text{O}_{12-\delta}$ samples. The most plausible reason for the improvement of these superconductivity parameters is the optimal carriers concentration and increased superconducting volume fraction of the samples after oxygen post-annealing.

The variation in the real part of dielectric constant (ϵ'_r) of oxygen post-annealed $\text{Cu}_{0.5}\text{Tl}_{0.5}\text{Ba}_2\text{Ca}_3(\text{Cu}_{4-y}\text{Cd}_y)\text{O}_{12-\delta}$ samples as a function of frequency at various temperatures in the range of 80–300 K is shown in Fig. 2(a–d). The portion of energy stored within the material of the sample is given by ϵ'_r , when exposed to electric field. The negative value of ϵ'_r is

Table 1

The comparison of superconductivity and dielectric properties of as-prepared and oxygen post-annealed $\text{Cu}_{0.5}\text{Tl}_{0.5}\text{Ba}_2\text{Ca}_3(\text{Cu}_{4-y}\text{Cd}_y)\text{O}_{12-\delta}$ ($y=0, 0.25, 0.5, \text{ and } 0.75$) superconductor samples.

y	$T_c(R=0)$ (K)	ϵ'_r at 10 kHz		ϵ''_r at 10 kHz		tan δ		σ_{ac} ($\Omega \text{ cm}$) ⁻¹	
		As-prepared	Oxygen post-annealed	As-prepared 80–300 K	Oxygen post-annealed 80–300 K	As-prepared 80–300 K	Oxygen post-annealed 80–300 K	As-prepared 80–300 K	Oxygen post-annealed 80–300 K
0	109	120	-3.7×10^6 to -2.6×10^5	1.04×10^9 – 2.23×10^8	2.39×10^8 – 1.79×10^7	300–1205	265–1323	577–124	133–10
0.25	107	114	-4.9×10^5 to -2.8×10^4	1.5×10^8 – 2.7×10^7	1.63×10^8 – 2.50×10^7	286–894	223–1449	83–15	60–11
0.5	102	115	-3.5×10^5 to -2.7×10^4	1.4×10^8 – 1.9×10^7	3.30×10^8 – 2.00×10^7	258–786	165–1802	50–12	42–14
0.75	82	85	-6.6×10^5 to -5.02×10^4	8.9×10^7 – 2.2×10^7	1.43×10^8 – 1.91×10^7	32–684	728–2260	40–11	28–11

calculated from the negative capacitance (NC) and the term NC reflects a decrease in sample capacitance from the geometric capacitance without the sample. This is most probably due to the development of positive space charge in the neighborhood of the electrodes. The positive space charge is most likely accumulated at the outer surface of the device

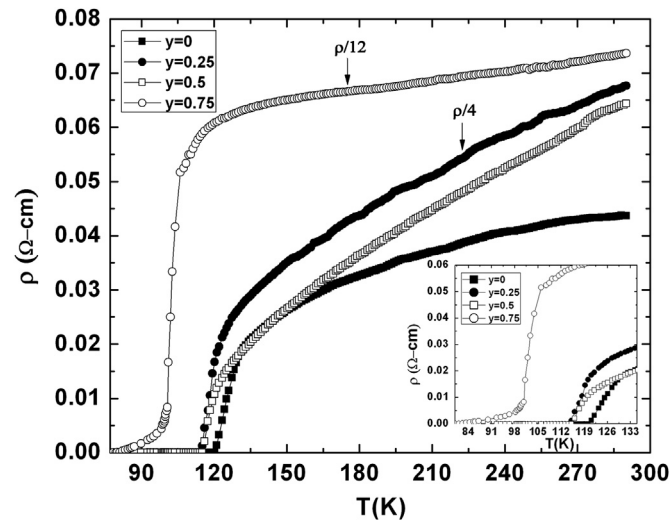


Fig. 1. The resistivity versus temperature measurements of oxygen post-annealed $\text{Cu}_{0.5}\text{Tl}_{0.5}\text{Ba}_2\text{Ca}_3(\text{Cu}_{4-y}\text{Cd}_y)\text{O}_{12-\delta}$ ($y=0, 0.25, 0.5,$ and 0.75) superconductor samples.

because the free negative charge carriers (electrons) flow toward the metal electrodes from the ceramic sample. As the Fermi level of the ceramics is at higher energy than that of metals, therefore, the migration of electrons from ceramics to metal surface is possible; the ceramics have less filled states than metals. The NC was observed in the samples with metal–semiconductor interfaces in the low frequency ranges [18–23]. The NC was also observed in some other materials [24–26]. The reasons of NC mechanism are different in different materials. In these studies, it is reported that the microscopic phenomena associated with NC at the metal–semiconductor interface includes the trapping of carriers (capture and emission), space charge effects and contact injection [18,27]. The maximum values of ϵ'_r in oxygen post-annealed $\text{Cu}_{0.5}\text{Tl}_{0.5}\text{Ba}_2\text{Ca}_3(\text{Cu}_{4-y}\text{Cd}_y)\text{O}_{12-\delta}$ samples at frequency of 10 KHz and in temperature range of 80–300 K are around from -2.06×10^6 to -1.03×10^4 , -3.52×10^5 to -2.34×10^4 , -3.38×10^5 to -4.27×10^3 and -3.49×10^4 to -1.33×10^3 for $y=0, 0.25, 0.5,$ and 0.75 respectively. The maximum values of ϵ'_r in all $\text{Cu}_{0.5}\text{Tl}_{0.5}\text{Ba}_2\text{Ca}_3(\text{Cu}_{4-y}\text{Cd}_y)\text{O}_{12-\delta}$ samples is decreased after oxygen post-annealing, Fig. 2(a–d).

The imaginary part of the dielectric constant (ϵ''_r) gives the absorption and attenuation of energy across the interfaces under the applied external electric field. The interfaces include grain boundaries, localized defects and localized charge densities at the defects sites. The variation of ϵ''_r versus $\text{Log}\{f(\text{Hz})\}$ at various temperatures from 80–300 K of oxygen

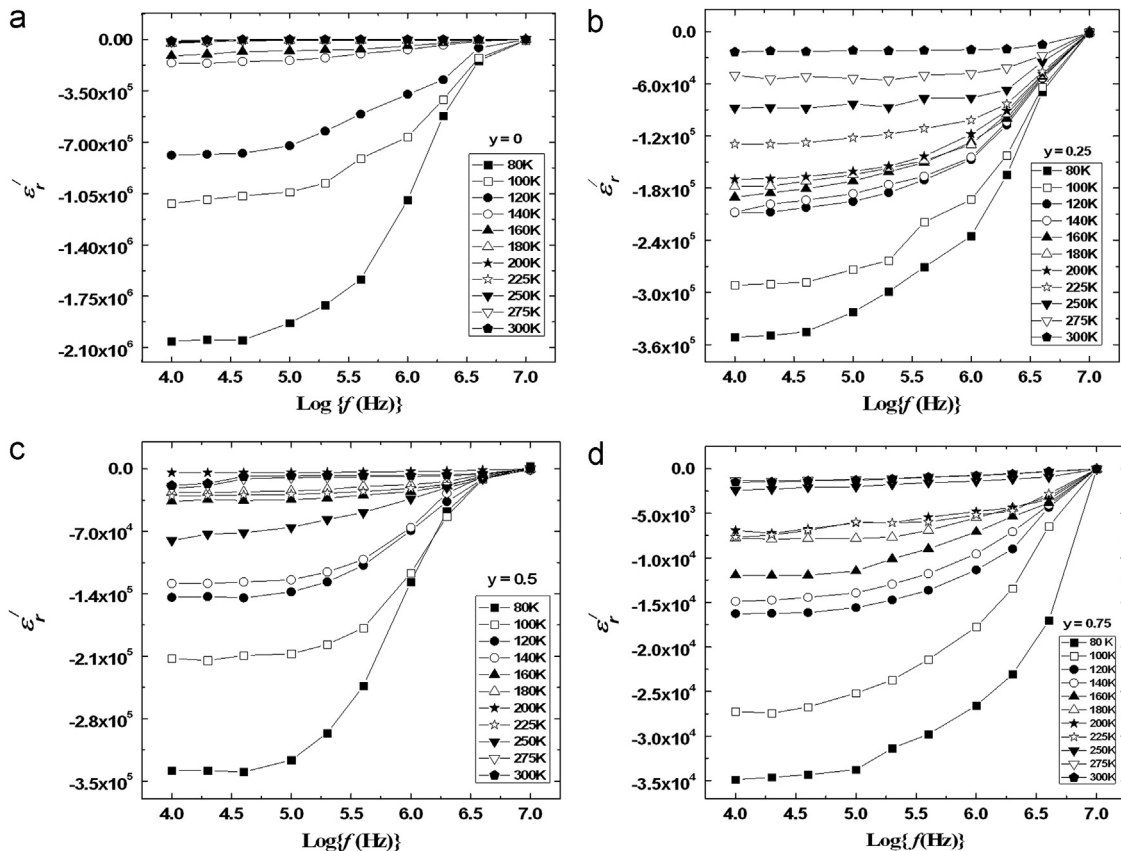


Fig. 2. (a–d). The dielectric constant (ϵ'_r) versus log of the frequency $\{\text{Log}\{f(\text{Hz})\}$ of the external field applied on oxygen post-annealed $\text{Cu}_{0.5}\text{Tl}_{0.5}\text{Ba}_2\text{Ca}_3(\text{Cu}_{4-y}\text{Cd}_y)\text{O}_{12-\delta}$ (a) $y=0,$ (b) $y=0.25,$ (c) $y=0.5,$ and (d) $y=0.75,$ superconductor samples.

post-annealed $\text{Cu}_{0.5}\text{Tl}_{0.5}\text{Ba}_2\text{Ca}_3(\text{Cu}_{4-y}\text{Cd}_y)\text{O}_{12-\delta}$ samples, Fig. 3(a–d). The maximum values of ϵ''_r are around from 2.39×10^8 to 1.79×10^7 , 1.63×10^8 to 2.50×10^7 , 3.30×10^8 to 2.00×10^7 and 1.43×10^8 to 1.91×10^7 at 80–300 K and 10 KHz for $y=0, 0.25, 0.5,$ and $0.75,$ respectively, after oxygen post-annealing. The less attenuation in energy is observed after oxygen post-annealing that may be due to large intake of oxygen in the $\text{Cu}_{0.5}\text{Tl}_{0.5}\text{Ba}_2\text{O}_{4-\delta}$ charger reservoir layer. The large intake of oxygen may change the charge state of Tl from (3+) to (1+) in $\text{Cu}_{0.5}\text{Tl}_{0.5}\text{Ba}_2\text{O}_{4-\delta}$ charger reservoir layer that reduces the localization of carriers resulting in the decrease in the dielectric properties after oxygen post-annealing [28,29].

The values of ϵ'_r and ϵ''_r in $\text{Cu}_{0.5}\text{Tl}_{0.5}\text{Ba}_2\text{Ca}_3(\text{Cu}_{4-y}\text{Cd}_y)\text{O}_{12-\delta}$ samples are much less than those observed in $\text{Tl}_2\text{Ba}_2\text{Ca}_2\text{Cu}_3\text{O}_x$ (Tl-2223) and $\text{Tl}_2\text{Ba}_2\text{Ca}_1\text{Cu}_2\text{O}_x$ (Tl-2212) superconductor samples [6]. The values of the dielectric constants observed in $\text{Cu}_{0.5}\text{Tl}_{0.5}\text{Ba}_2\text{Ca}_3(\text{Cu}_{4-y}\text{Cd}_y)\text{O}_{12-\delta}$ samples are even much smaller than those values observed in Nd-doped $\text{Bi}_2\text{Ba}_2\text{Nd}_{1.6}\text{Ce}_{0.4}\text{Cu}_3\text{O}_{10-\delta}$ and Bi–Pb–Sr–Ca–Cu–O superconductors [8,30]. A significant difference in the values of ϵ'_r and ϵ''_r may possibly be due to larger difference in the thickness of charge reservoir layer; $\text{Tl}_2\text{Ba}_2\text{O}_{5-\delta}$ charge reservoir layer of double Tl layer compounds is thicker as compared to $\text{TlBa}_2\text{O}_{4-\delta}$ charge reservoir layer of single Tl layer compounds. Moreover, $(\text{Cu}_{0.5}\text{Tl}_{0.5})\text{Ba}_2\text{O}_{4-\delta}$ charge reservoir layer in $\text{Cu}_{0.5}\text{Tl}_{0.5}\text{Ba}_2\text{Ca}_3(\text{Cu}_{4-y}\text{Cd}_y)\text{O}_{12-\delta}$

superconductor is more conducting, whereas, $\text{Tl}_2\text{Ba}_2\text{O}_{5-\delta}$ charge reservoir layer in Tl-2223 and Tl-2212 superconductors is insulating [7]. The former supplies more carriers to the conducting $\text{CuO}_2/\text{CdO}_2$ planes as compared to the totally insulating $\text{Tl}_2\text{Ba}_2\text{O}_{5-\delta}$ charge reservoir layers. Naturally lower values of capacitance are observed in $\text{Cu}_{0.5}\text{Tl}_{0.5}\text{Ba}_2\text{Ca}_3(\text{Cu}_{4-y}\text{Cd}_y)\text{O}_{12-\delta}$ samples as compared to Tl-2223 and Tl-2212 samples, whereas a higher conductance is observed in our samples as compared to double layered thallium based superconductors. In Bi-2212, Bi-2223, Tl-2223 and Tl-2212 compounds, the $\text{M}_2\text{Ba}_2\text{O}_{5-\delta}$ (M=Bi, Tl) charge reservoir layers contain trivalent Bi^{3+} and Tl^{3+} ions [7,8,30]. These trivalent ions may localize the carriers at their own sites and can suppress carriers flow to the conducting CuO_2 planes. But the $\text{Cu}_{0.5}\text{Tl}_{0.5}\text{Ba}_2\text{O}_{4-\delta}$ charge reservoir layer of our $\text{Cu}_{0.5}\text{Tl}_{0.5}\text{Ba}_2\text{Ca}_3(\text{Cu}_{4-y}\text{Cd}_y)\text{O}_{12-\delta}$ compound has partially insulating/conducting character due to the presence of Cu atoms, which most likely enhances their doping efficiency. The change in the dielectric constants of $\text{Cu}_{0.5}\text{Tl}_{0.5}\text{Ba}_2\text{Ca}_3(\text{Cu}_{4-y}\text{Cd}_y)\text{O}_{12-\delta}$ samples is due to the variation of O_δ in $\text{Cu}_{0.5}\text{Tl}_{0.5}\text{Ba}_2\text{O}_{4-\delta}$ charge reservoir layer after oxygen post-annealing [15].

The ratio of energy dissipated and energy stored in the material determines the dielectric loss factor ($\tan \delta$) and the absolute value of dielectric loss factor $|\tan \delta|$ versus $\text{Log}\{f(\text{Hz})\}$ of the oxygen post-annealed $\text{Cu}_{0.5}\text{Tl}_{0.5}\text{Ba}_2\text{Ca}_3(\text{Cu}_{4-y}\text{Cd}_y)\text{O}_{12-\delta}$ samples are shown in Fig. 4(a–d). The

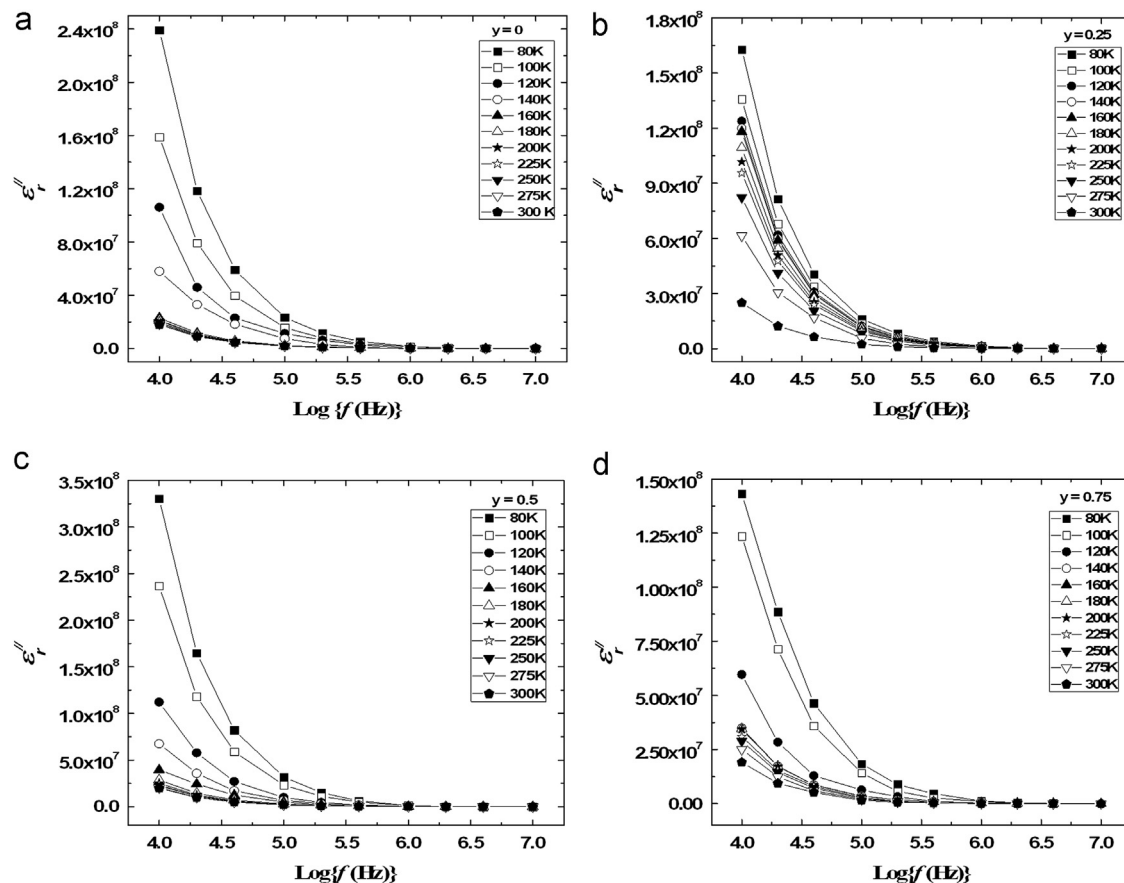


Fig. 3. (a–d). The imaginary part of dielectric (ϵ''_r) versus log of the frequency $\{\text{Log}f(\text{Hz})\}$ of the external field applied on oxygen post-annealed $\text{Cu}_{0.5}\text{Tl}_{0.5}\text{Ba}_2\text{Ca}_3(\text{Cu}_{4-y}\text{Cd}_y)\text{O}_{12-\delta}$ (a) $y=0,$ (b) $y=0.25,$ (c) $y=0.5,$ and (d) $y=0.75,$ superconductor samples.

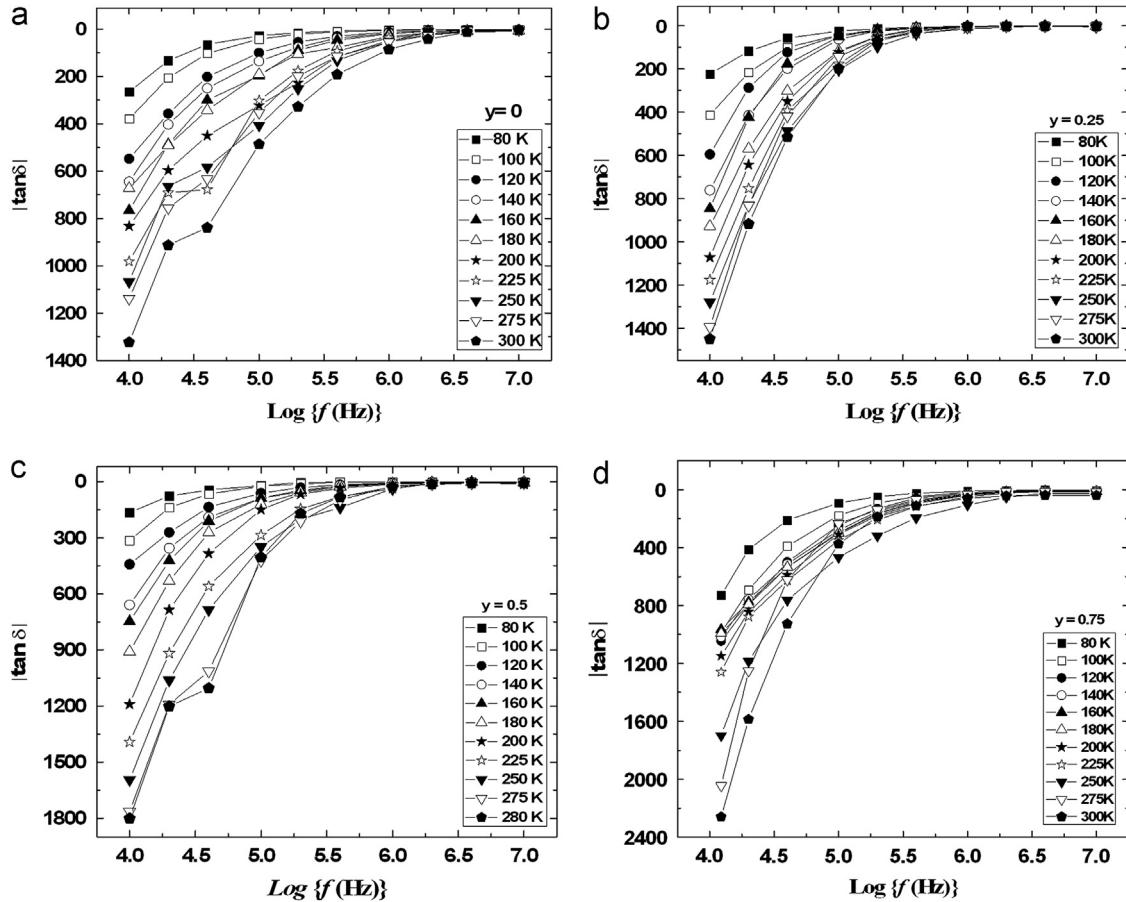


Fig. 4. (a–d). The absolute dielectric loss $|\tan \delta|$ versus log of the frequency $\{\text{Log } f(\text{Hz})\}$ of the external field applied on oxygen post-annealed $\text{Cu}_{0.5}\text{Tl}_{0.5}\text{Ba}_2\text{Ca}_3(\text{Cu}_{4-y}\text{Cd}_y)\text{O}_{12-\delta}$ (a) $y=0$, (b) $y=0.25$, (c) $y=0.5$, and (d) $y=0.75$, superconductor samples.

values of $|\tan \delta|$ are observed around 265–1323, 223–1449, 165–1802 and 728–2260 at 10 kHz and temperature range from 80 to 300 K for $y=0$, 0.25, 0.5, and 0.75, respectively, after oxygen post-annealing $\text{Cu}_{0.5}\text{Tl}_{0.5}\text{Ba}_2\text{Ca}_3(\text{Cu}_{4-y}\text{Cd}_y)\text{O}_{12-\delta}$ samples. The dielectric loss has increased in all $\text{Cu}_{0.5}\text{Tl}_{0.5}\text{Ba}_2\text{Ca}_3(\text{Cu}_{4-y}\text{Cd}_y)\text{O}_{12-\delta}$ samples after oxygen post-annealing. The increase in the value of $|\tan \delta|$ is the conjuncture of oxygen intake after post-annealing in oxygen, which may increase the thickness of the charge reservoir layer and hence the dielectric loss.

The ac-conductivity (σ_{ac}) versus $\text{Log}\{f(\text{Hz})\}$ measurements of oxygen post-annealed $\text{Cu}_{0.5}\text{Tl}_{0.5}\text{Ba}_2\text{Ca}_3(\text{Cu}_{4-y}\text{Cd}_y)\text{O}_{12-\delta}$ samples have been shown in Fig. 5(a–d). The values of σ_{ac} are observed around 133–10, 60–11, 42–14 and 28–11 for $y=0$, 0.25, 0.5, and 0.75, respectively, at 10 kHz and in the temperature range of 80–300 K after oxygen post-annealing of $\text{Cu}_{0.5}\text{Tl}_{0.5}\text{Ba}_2\text{Ca}_3(\text{Cu}_{4-y}\text{Cd}_y)\text{O}_{12-\delta}$ samples. The value of σ_{ac} was decreased significantly in all $\text{Cu}_{0.5}\text{Tl}_{0.5}\text{Ba}_2\text{Ca}_3(\text{Cu}_{4-y}\text{Cd}_y)\text{O}_{12-\delta}$ samples after oxygen post-annealing. The density of the phonon population is suppressed due the damped harmonic oscillations of heavier Cd atoms in the CuO_2 planes, which reduces the magnitude of superconductivity in the final compound [31]. But after oxygen post-annealing the value of T_c ($R=0$) is increased, which is most likely due to

optimization of oxygen in $\text{Cu}_{0.5}\text{Tl}_{0.5}\text{Ba}_2\text{O}_{4-\delta}$ charge reservoir layer that optimizes the density of carriers in the conducting planes [15].

These materials with giant dielectric constant are playing an increasingly significant role in the race of microelectronics because of the desire for small and more robust devices such as capacitors and memory devices [32]. However, the main obstacle for potential applications as dielectrics is the high conductivity of cuprates, which results in high dissipation loss. To increase the dielectric constant and to reduce the dissipation loss in superconductors is an open question for all the scientific community.

4. Conclusion

We have investigated the effects of oxygen post-annealing on the superconductivity and dielectric properties of $\text{Cu}_{0.5}\text{Tl}_{0.5}\text{Ba}_2\text{Ca}_3(\text{Cu}_{4-y}\text{Cd}_y)\text{O}_{12-\delta}$ superconductor samples. The negative capacitance (NC) has been observed in all oxygen post-annealed $\text{Cu}_{0.5}\text{Tl}_{0.5}\text{Ba}_2\text{Ca}_3(\text{Cu}_{4-y}\text{Cd}_y)\text{O}_{12-\delta}$ samples. The change in the dielectric parameters after oxygen post-annealing is the evidence of the variation in O_δ oxygen of $\text{Cu}_{0.5}\text{Tl}_{0.5}\text{Ba}_2\text{O}_{4-\delta}$ charge reservoir layer that controls the flow of carriers toward the conducting CuO_2 planes. It is observed

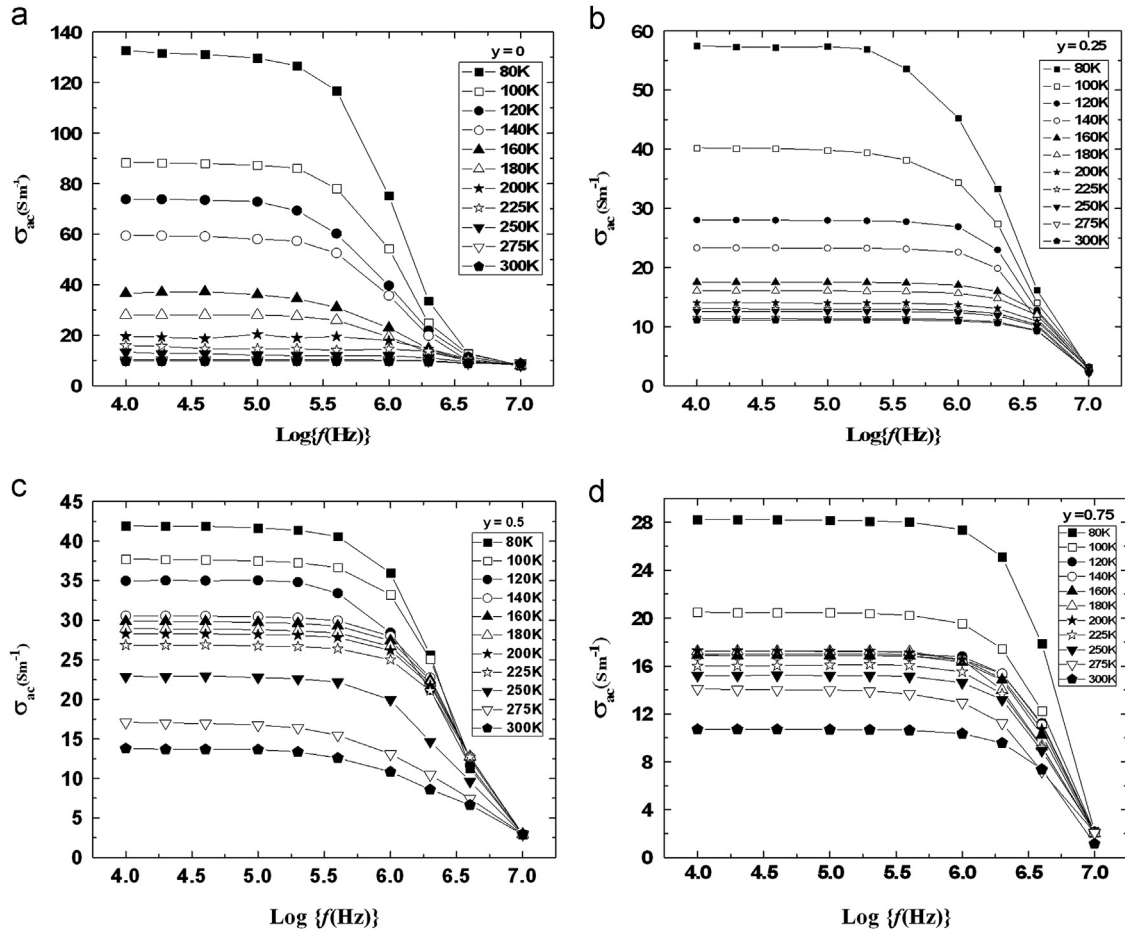


Fig. 5. (a–d). The ac-conductivity versus log of the frequency $\{\text{Log}\{f(\text{Hz})\}$ of the external field applied on oxygen post-annealed $\text{Cu}_{0.5}\text{Tl}_{0.5}\text{Ba}_2\text{Ca}_3(\text{Cu}_{4-y}\text{Cd}_y)\text{O}_{12-\delta}$ (a) $y=0$, (b) $y=0.25$, (c) $y=0.5$, and (d) $y=0.75$, superconductor samples.

that the dielectric properties (ϵ'_r , ϵ''_r , and σ_{ac}) are decreased, while $\text{Im}\{\tan \delta\}$ is increased in $\text{Cu}_{0.5}\text{Tl}_{0.5}\text{Ba}_2\text{Ca}_3(\text{Cu}_{4-y}\text{Cd}_y)\text{O}_{12-\delta}$ samples after oxygen post-annealing. The variation in O_δ of $\text{Cu}_{0.5}\text{Tl}_{0.5}\text{Ba}_2\text{O}_{4-\delta}$ charge reservoir layer after oxygen post-annealing changes the dielectric properties of $\text{Cu}_{0.5}\text{Tl}_{0.5}\text{Ba}_2\text{Ca}_3(\text{Cu}_{4-y}\text{Cd}_y)\text{O}_{12-\delta}$ samples. The large intake of oxygen is reflected from appreciable change in the dielectric properties of $\text{Cu}_{0.5}\text{Tl}_{0.5}\text{Ba}_2\text{Ca}_3(\text{Cu}_{4-y}\text{Cd}_y)\text{O}_{12-\delta}$ samples after oxygen post-annealing. At normal state temperature (300 K), the thermal agitation is higher and polarizability is lower resulting in the decrease of dielectric constant and increase in dielectric loss factor. A strong dielectric dispersion is observed at low frequencies and temperatures and the reverse effects are observed on dielectric properties at higher frequencies and temperatures. The observed variations in the dielectric parameters of $\text{Cu}_{0.5}\text{Tl}_{0.5}\text{Ba}_2\text{Ca}_3(\text{Cu}_{4-y}\text{Cd}_y)\text{O}_{12-\delta}$ samples strongly depend on the working (or operating) temperature and frequency of the external applied ac-field. The dielectric behavior of the materials can be regulated by the oxygen post-annealing as a result of which the variation of oxygen content in the structure of the materials controls the carrier's density. Therefore, the oxygen post-annealing can be used as a tuning technique of these frequency and temperature dependent dielectric properties of $\text{Cu}_{0.5}\text{Tl}_{0.5}\text{Ba}_2\text{Ca}_3(\text{Cu}_{4-y}\text{Cd}_y)\text{O}_{12-\delta}$

superconducting samples. On the other hand, this oxygen post-annealing may affect the inter-grain connectivity of the material.

References

- [1] A. Iyo, Y. Tanaka, Y. Ishiura, M. Tokumoto, K. Tokiwa, T. Watanabe, H. Ihara, Study on enhancement of T_c (≥ 130 K) in $\text{TlBa}_2\text{Ca}_2\text{Cu}_3\text{O}_y$ superconductors, *Superconductor Science and Technology* 14 (2001) 504.
- [2] K. Tanaka, A. Iyo, N. Terada, K. Tokiwa, S. Miyashita, Y. Tanaka, T. Tsukamoto, S.K. Agarwal, T. Watanabe, H. Ihara, Tl valence change and T_c enhancement (> 130 K) in $(\text{Cu}, \text{Tl})\text{Ba}_2\text{Ca}_2\text{Cu}_3\text{O}_y$ due to nitrogen annealing, *Physical Review B* 63 (2001) 64508.
- [3] Nawazish A. Khan, M. Mumtaz, A.A. Khurram, Frequency dependent dielectric properties of $\text{Cu}_{0.5}\text{Tl}_{0.5}\text{Ba}_2\text{Ca}_2\text{Cu}_{3-y}\text{Zn}_y\text{O}_{10-\delta}$ ($y=0, 1.0, 1.5, 2.0, 2.5$) superconductors, *Journal of Applied Physics* 104 (2008) 033916.
- [4] Ş Çavdar, H Koralay, N Tuğluoğlu, A Günen, Frequency dependent dielectric characteristics of Tl–Ba–Ca–Cu–O bulk superconductor, *Superconductor Science and Technology* 18 (2005) 1204.
- [5] P. Ben Ishai, E. Sader, Yu. Feldman, I. Felner, M. Weger, Dielectric properties of $\text{Na}_{0.7}\text{CoO}_2$ and of the Superconducting $\text{Na}_{0.3}\text{CoO}_2 \cdot 1.3\text{H}_2\text{O}$, *Journal of Superconductivity* 18 (2005) 455.
- [6] M. Nikolo, R.B. Goldfarb, Flux creep and activation energies at the grain boundaries of Y–Ba–Cu–O superconductors, *Physical Review B* 39 (1989) 6615.
- [7] J.S. Blakemore, *Solid State Physics*, Second Edition, Cambridge University Press, New York 412.

- [8] L.L. Hench, J.K. West, *Principles of Electronic Ceramics*, Wiley, New York, NY, USA, 1990.
- [9] Lu Li, C. Richter, S. Paetel, T. Kopp, J. Mannhart, R.C. Ashoori, Very Large capacitance enhancement in a two-dimensional electron system, *Science* 332 (2011) 825.
- [10] A.A. Khurram, M. Mumtaz, Nawazish A. Khan, M.M. Ahadian, Azam Irajizad, The effect of grain size on the fluctuation-induced conductivity of $\text{Cu}_{1-x}\text{Tl}_x\text{Ba}_2\text{Ca}_3\text{Cu}_4\text{O}_{12-\delta}$ superconductor thin films, *Superconductor Science and Technology* 20 (2007) 742.
- [11] S. Mikusu, N. Urita, Y. Hashinaka, K. Tokiwa, A. Iyo, Y. Tanaka, T. Watanabe, Transport properties of $\text{TlBa}_2\text{Ca}_2\text{Cu}_3\text{O}_y$ in an over-doped state, *Physica C* 442 (2006) 91.
- [12] J.Y. Juang, J.H. Horng, S.P. Chen, C.M. Fu, K.H. Wu, T.M. Uen, Y.S. Gou, Enhancement of critical current density in direct-current-sputtered $\text{TlBa}_2\text{Ca}_2\text{Cu}_3\text{O}_{9 \pm \delta}$ superconducting thin films, *Applied Physics Letters* 66 (1995) 885.
- [13] Z.X. Cheng, X.L. Wang, S. Keshavarzi, M.J. Qin, T.M. Silver, H.K. Liu, H. Kimura, S.X. Dou, The morphology, periodical modulation structure and effects of heat treatment on the superconductivity of (Tl, Pb)(Sr, Ba)-1223 single crystals, *Superconductor Science and Technology* 17 (2004) 696.
- [14] R.T. Lu, S.L. Yan, L. Fang, M. He, Enhanced superconductivity in $\text{TlBa}_2\text{CaCu}_2\text{O}_x$ thin films by the variation of oxygen content, *Superconductor Science and Technology* 14 (2001) 948.
- [15] M. Rahim, Nawazish A. Khan, M. Mumtaz, Temperature and frequency dependent dielectric properties of $\text{Cu}_{0.5}\text{Tl}_{0.5}\text{Ba}_2\text{Ca}_3(\text{Cu}_{4-y}\text{Cd}_y)\text{O}_{12-\delta}$ bulk superconductor, *Journal of Low Temperature Physics* (2012) <http://dx.doi.org/10.1007/s10909-012-0840-z> (2013).
- [16] M.S. Vijaya, G. Rangarajan, *Materials Science*, 1st ed., Tata McGraw-Hill Publishing Company Ltd., New Delhi, India, 2004.
- [17] Nawazish A. Khan, M. Rahim, Superconducting properties of Cd doped $\text{Cu}_{0.5}\text{Tl}_{0.5}\text{Ba}_2\text{Ca}_3\text{Cu}_{4-y}\text{Cd}_y\text{O}_{12-\delta}$ ($y=0, 0.25, 0.5, 0.75, 1.0$) superconductors, *Journal of Alloys and Compounds* 481 (2009) 81.
- [18] G.B. Parravicini, A. Stella, M.C. Ungureanu, R. Kofman, Low frequency negative capacitance effect in systems of metallic nanoparticles embedded in dielectric matrix, *Applied Physics Letters* 85 (2004) 302.
- [19] M. Ershov, H.C. Liu, L. Li, M. Buchanan, Z.R. Wasilewski, A.K. Jonscher, Negative capacitance effect in semiconductor devices, *IEEE Transactions on Electron Devices* 45 (1998) 2196.
- [20] N.A. Penin, Negative capacitance in semiconductor structures, *Semiconductors* 30 (1996) 340.
- [21] A.K. Jonscher, The physical origin of negative capacitance, *Journal of the Chemical Society* 82 (1986) 75.
- [22] M. Beale, P. Mackay, The origins and characteristics of negative capacitance in metal–insulator–metal devices, *Philosophical Magazine B* 65 (1992) 47.
- [23] J.C.M. Peko, Effect of negative capacitances on high-temperature dielectric measurements at relatively low frequency, *Applied Physics Letters* 71 (1997) 3730.
- [24] M. Ershov, H.C. Liu, L. Li, M. Buchanan, Z.R. Wasilewski, V. Ryzhii, Unusual capacitance behavior of quantum well infrared photodetectors, *Applied Physics Letters* 70 (1997) 1828.
- [25] N.C. Chen, P.Y. Wang, J.F. Chen, Low frequency negative capacitance behavior of molecular beam epitaxial GaAs n-low temperature-i-p structure with low temperature layer grown at a low temperature, *Applied Physics Letters* 72 (1998) 1081.
- [26] A.G.U. Perera, W.Z. Shen, M. Ershov, H.C. Liu, M. Buchanan, W. J. Schaff, Negative capacitance of GaAs homojunction far-infrared detectors, *Applied Physics Letters* 74 (1999) 3167.
- [27] B.S. Doyle, Anomalous low-frequency resonance-type behaviour and negative capacitance in doped glasses, *Journal of Physics D* 19 (1986) 1129.
- [28] H. Ihara, K. Tanaka, Y. Tanaka, A. Iyo, N. Terada, M. Tokumoto, F. Tateai, M. Kawamura, K. Ishida, S. Miyashita, T. Watanabe, Mechanism of T_c enhancement in $\text{Cu}_{1-x}\text{Tl}_x\text{-1234}$ and -1223 system with $T_c > 130$ K, *Physica C* 341-348 (2000) 487.
- [29] Nawazish A. Khan, M. Mumtaz, M.M. Ahadian, Azam Irajizad, X-ray photo-emission studies of $\text{Cu}_{1-x}\text{Tl}_x\text{Ba}_2\text{Ca}_3\text{Cu}_4\text{O}_{12-y}$ superconductor thin films, *Physica C* 449 (2006) 47.
- [30] R.K. Nkum, M.O. Gyekye, F. Boakye, Normal-state dielectric and transport properties of In-doped Bi–Pb–Sr–Ca–Cu–O, *Solid State Communications* 122 (2002) 569.
- [31] Asad Raza, M. Rahim, Nawazish A. Khan, Fluctuation induced conductivity analyses of Cd doped $\text{Cu}_{0.5}\text{Tl}_{0.5}\text{Ba}_2\text{Ca}_2\text{Cu}_{3-y}\text{Cd}_y\text{O}_{10-\delta}$ ($y=0, 0.5, 1.0, 1.5$) superconductors, *Ceramics International* 39 (2013) 4349.
- [32] X. Xu, Z. Jiao, M. Fu, L. Feng, K. Xu, R. Zuo, X. Chen, Dielectric studies in a layered Ba based Bi-2222 cuprate $\text{Bi}_2\text{Ba}_2\text{Nd}_{1.6}\text{Ce}_{0.4}\text{Cu}_2\text{O}_{10+\delta}$, *Physica C* 417 (2005) 166.